ODF were obtained for both sediment aggregates and evaporated thin films (Gemmi, Voltolini *et al.*, 2011).

2.4.6. Rietveld refinement with electron diffraction data

By T. E. Gorelik and U. Kolb

The Rietveld refinement method was initially developed for neutron diffraction data (Rietveld, 1967, 1969). It has now become a standard technique which is extensively used with neutron, laboratory X-ray and synchrotron diffraction data. A detailed description of the method can be found in Chapter 4.7.

Compared with the popularity of Rietveld refinement in X-ray and neutron powder diffraction, its application to powder electron diffraction data is very limited. So far, Rietveld refinement with electron diffraction data has only been done for nanocrystalline Al, α-MnS (Gemmi, Fischer *et al.*, 2011), hydroxyapatite (Song *et al.*, 2012), intermetallic AuFe (Luo *et al.*, 2011), TiO_2 (Weirich *et al.*, 2000; Tonejc *et al.*, 2002; Djerdj & Tonejc, 2005, 2006) and $MnFe_2O_4$ (Kim *et al.*, 2009). An example of a fit with powder electron diffraction data obtained by Rietveld refinement for hydroxyapatite is shown in Fig. 2.4.7.

Two major factors limit the application of Rietveld refinement to electron powder diffraction. First, electron powder diffraction data are collected from a sample volume far smaller than that used in an X-ray experiment. Therefore, the average statistics are poor compared with those of X-ray data. Nevertheless, electron powder diffraction data from a small sample area or thin films can give specific information which is difficult to obtain using other methods. Second, the presence of dynamical effects in the electron diffraction data hinders quantitative assessment of reflection intensities. Dynamical effects are strongest in zone-axis electron diffraction geometry, when many beams belonging to the same systematic rows are excited simultaneously. In powder electron diffraction crystals are randomly oriented towards the electron beam, thus making the fraction of zonal patterns low, thereby reducing the dynamical scattering in the data (see Section 2.4.2 for a more detailed discussion).

Within the limit of kinematical diffraction, the principle of Rietveld refinement is the same for electrons and X-rays, except the electron atomic scattering factors are different. The refinement procedure can thus be performed using existing programs if it is possible to input the scattering factors for electrons. Most of the reported Rietveld refinements on electron powder diffraction data have been performed using *FullProf* (Rodríguez-Carvajal, 1993); a refinement in *MAUD* (Lutterotti *et al.*, 1999) has also been reported (Gemmi, Voltolini *et al.*, 2011).

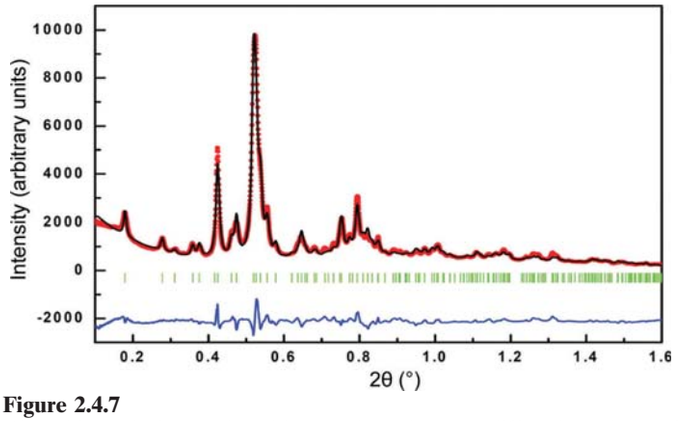

Figure 2.4.7
Rietveld analysis result with powder electron diffraction data of hydroxyapatite. Reproduced from Song *et al.* (2012) with permission from Oxford University Press.

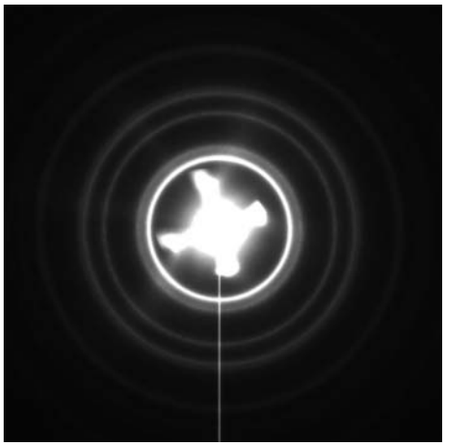

Figure 2.4.8
Powder electron diffraction pattern of nanocrystalline gold demonstrating non-symmetrical background features.

Electron powder diffraction patterns are recorded on an area detector. For a Rietveld refinement the two-dimensional diffraction patterns have to be integrated into one-dimensional profiles. The zero shift is treated as for the X-ray data integrated from a two-dimensional position-sensitive detector. Details about electron diffraction data processing and calibration are given in Section 2.4.3.4.

The background in electron powder patterns is a complex combination of inelastic scattering, scattering from the supporting film (when it is present) and other factors. For the Rietveld refinement procedure the background of a one-dimensional integrated profile is fitted by a polynomial function. If a supporting thin amorphous carbon film is used, the background can include broad rings, which after the one-dimensional integration can produce pronounced broad peaks. These peaks are difficult to subtract using a model based on a polynomial function; therefore, these intensities may hamper the powder diffraction profile matching (Kim *et al.*, 2009). In some cases, the background can even include radially non-symmetric features originating from the shape of the tip within the electron source (see Fig. 2.4.8); it can have blooming due to oversaturated CCD pixels, or streak shadows due to the fast transmission electron microscope beam-shutter movement. In these cases, a diffraction pattern from the adjacent 'empty' area of the sample can be acquired and subtracted from the diffraction pattern of the material prior to the integration into one dimension. This procedure allows elimination of some of the artifacts discussed above, which otherwise after the one-dimensional integration may be falsely interpreted as diffraction peaks, and are generally more difficult to fit.

Unit-cell parameters are mostly subject to the error due to the accuracy of the electron diffraction camera-length calibration. Although examples have been published showing 0.3% accuracy of the camera-length calibration, in most cases accuracy of about 2% can be achieved (Williams & Carter, 2009). The effective camera length depends on many instrumental parameters such as the convergence of the electron beam, the diffraction lens focus, the mechanical position of the sample within the objective lens, or the hysteresis of the electromagnetic lenses. Thus, while the ratio of the lattice parameters within one aligned diffraction pattern can be very precise, the absolute values might not be.

Atomic displacement parameters can be refined from electron powder diffraction data; however, the interpretation of the results can be manifold. For nanocrystalline materials, which have a relatively high surface-to-volume ratio, the surface effect can be enhanced compared with that of the bulk. Thus, the average atomic displacement factors can increase because of the high fraction of near-surface relaxed atoms. Consequently, the isotropic displacement parameter B resulting from the Rietveld refinement can be relatively high. Local heating (Reimer, 1984) during the electron illumination may also contribute to higher average displacement parameters. Finally, if the electron beam exceeds a material-dependent threshold acceleration voltage, it can cause knock-on damage (Williams & Carter, 2009) in both organic and inorganic materials. This is a dynamical process which can cause both material loss and rearrangement of atoms. The presence of defects resulting from the rearrangement of atoms may lead to an increase in the average displacement factors. Nevertheless, the refinement using polycrystalline anatase data showed the expected displacement parameters of 1.4 (1) Å^2 for Ti and 1.9 (2) Å^2 for oxygen (Weirich *et al.*, 2000). Of all the parameters used during Rietveld refinement, the displacement parameters and atomic coordinates are probably the most sensitive to a possible dynamical-scattering contribution in the data. It is noticeable that after the refinement of the anatase structure the atomic coordinates converged to reasonable positions: [0, $\frac{1}{4}$, 0.1656 (5)] for oxygen (Weirich *et al.*, 2000) compared with the previous range obtained in neutron diffraction studies of [0, $\frac{1}{4}$, 0.16686 (5)] (Burdett *et al.*, 1987) to [0, $\frac{1}{4}$, 0.20806 (5)] (Howard *et al.*, 1991).

The relative ratio of two components in a mixture can be determined using the Hill–Howard approach (Hill & Howard, 1987): the relative weight of a phase in a mixture of phases is proportional to the scaling factor of the phase given by the Rietveld refinement combined with the mass and the volume of the unit cell of the component. The relative content of a mixture of anatase and brookite was successfully determined from electron powder diffraction data (Djerdj & Tonejc, 2005, 2006).

For the modelling of the Bragg reflection shape the Pearson VII function can be used (Weirich *et al.*, 2000; Kim *et al.*, 2009), although recently the more popular pseudo-Voigt peak shape function has been used (Tonejc *et al.*, 2002; Djerdj & Tonejc, 2005, 2006) and provides a satisfactory fit between the experimental and calculated data.

The average crystalline domain size can be determined using line-broadening analysis. The measured intensity profile is a convolution of the physical line profile given by the sample with the instrumental profile broadening. When expressed in terms of the scattering angle θ, the width of the electron diffraction peaks is much smaller than that for X-rays. On the other hand, electrons generally have a smaller coherence length than X-rays. As a result, for the same material, the effective peak width for electron diffraction is larger than that for powder X-ray data (Song *et al.*, 2012). Because of this, it is sometimes difficult to separate the domain size and the instrumental contributions to the peak broadening. Therefore, the average domain size obtained after the refinement procedure should be cross-checked with the domain size determined from TEM images obtained, for instance, using the dark-field technique (Williams & Carter, 2009).

In electron diffraction various instrumental parameters can affect the peak width. The energy spread of the electrons causes additional broadening of diffracted spots. This effect can be partially reduced by energy filtering of the diffraction patterns (Kim *et al.*, 2009; Egerton, 2011). Finally, the electron diffraction camera length must be large enough that the detector broadening is much smaller than the peak width, as demonstrated in Fig. 2.4.9: large values of the camera length ('zoomed in' diffraction patterns) result in thinner, better separated peaks.

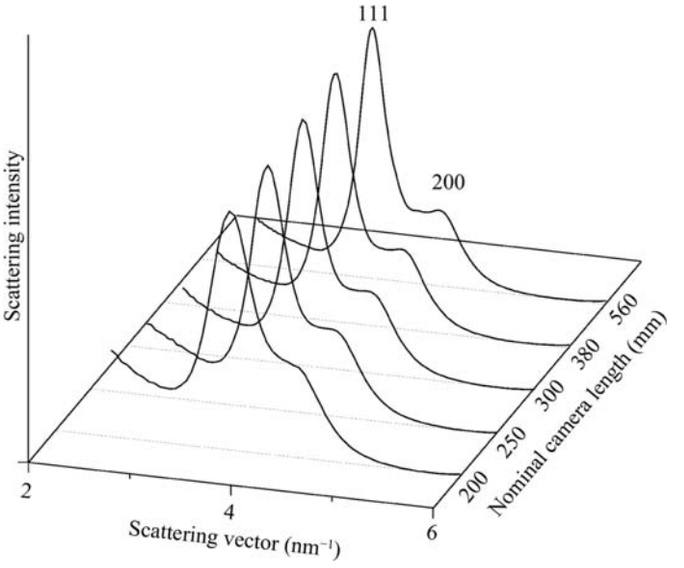

Figure 2.4.9
Electron powder diffraction profiles of gold nanoparticles (range 2–6 nm^{-1}) recorded at different electron diffraction camera lengths.

Preferred orientation can be an issue for electron powder diffraction: when the powder material is supported on a thin film, the crystals tend to orient themselves with their most developed facet facing the support. As a result, the relative intensities of the diffracted peaks are modified (Kim *et al.*, 2009). Texture within nanocrystalline powders introduced by the sample preparation on a support for TEM can be analysed using electron powder diffraction patterns recorded at different tilt positions of the sample. Refinement of the preferred orientation of two different materials – nanocrystalline aluminium and α-MnS powders – showed that the aluminium particles tend to have strong preferred orientation due to their facet morphology, while α-MnS particles are randomly oriented (Gemmi, Fischer *et al.*, 2011).

Although dynamical effects are believed to be reduced for nanocrystalline materials and additionally reduced by data collection from non-oriented crystals, the dynamical component of the scattering cannot be neglected. For the dynamical correction using the two-beam approximation formalism of equation (2.4.12), the reader is referred to Section 2.4.2. For a range of electron-beam energies from 20 to 50 kV it has been shown that polycrystalline electron diffraction patterns of aluminium crystals smaller than 9 nm have a dynamical scattering component below 10% (Horstmann & Meyer, 1962). For polycrystalline $MnFe_2O_4$ with an average crystal size of 11 nm measured using a 120 kV electron beam, the ratio of the kinematical to dynamical contributions in the structure factor was about 1:1.5 (Kim *et al.*, 2009). The application of the small (less than 3%) correction for the dynamical component during Rietveld refinement of nanocrystalline intermetallic Au_3Fe_{1-x} improved the refined long-range order parameter of the alloy (Luo *et al.*, 2011).

In summary, the Rietveld refinement technique applied to electron powder diffraction data is a new area of research. It can be successfully carried out for small volumes of nanocrystalline materials, for which the small electron beam is an advantage. Results obtained from Rietveld analysis of electron powder

diffraction data of nanocrystalline materials are encouraging. The refinement for powders containing large crystal grains is problematic because of dynamical scattering present in the data. There are also uncertainties caused by instrumental effects. The dynamical effects can be accounted for using the Blackman formalism, while the influence of diverse instrumental parameters needs further systematic study.

2.4.7. The pair distribution function from electron diffraction data

By T. E. Gorelik and U. Kolb

An extensive description of pair distribution function (PDF) analysis covering data acquisition, reduction and interpretation can be found in Chapter 5.7. Here, only a short outline is presented, concentrating on aspects that are specific to PDFs obtained by electron diffraction.

Poorly crystalline and amorphous materials exhibit no long-range order and therefore show no pronounced Bragg peaks in diffraction patterns. Nevertheless, owing to defined bonding geometry, these materials do have a specific local arrangement of atoms, denoted as short-range order. The short-range order can be analysed using the PDF obtained from the total scattering profile. The PDF can provide general information about the degree of order, the character of local atomic packing and the size of the correlation domains. The total scattering function is collected over a wide range of reciprocal space and includes not only the Bragg reflections (if present), but also the diffuse scattering information between them (Egami & Billinge, 2003).

The PDF $G(r)$ represents the probability of finding a pair of atoms with an interatomic distance r, weighted by the scattering power of the individual atoms. After normalization and suitable corrections, the reduced scattering function $F(Q)$ is derived. [In the PDF analysis, the scattering vector Q, which is related to the scattering angle θ as $Q = (4\pi \sin\theta)/\lambda$ is used, instead of $S = \sin\theta/\lambda$.] The PDF can be calculated by the Fourier transformation of $F(Q)$ into direct space (Warren, 1990; Egami & Billinge, 2003; Farrow & Billinge, 2009).

Powder diffraction data for PDF analysis should be measured over a sufficiently large range of the scattering angle θ; therefore, neutron or synchrotron sources or laboratory X-ray data with a short-wavelength source (Mo or Ag anode) are used. Powder electron diffraction data, with their flexibility in electron diffraction camera length, short wavelength and nuclear scattering at large scattering angles, can also cover the desired large range of scattering angles and are therefore highly suitable for PDF analysis. In addition, atoms have a much larger scattering cross section for electrons than for X-rays or neutrons, allowing sufficient signal collection from very small volumes. Finally, electrons can be focused with lenses down to a few nanometres. All these reasons make electron diffraction analysis attractive for the study of the structure of nanovolumes. The electron PDF is therefore a powerful tool for the investigation of the structures of amorphous or poorly crystalline thin films, or for small sample volumes of inhomogeneous samples.

There are several practical issues to consider when collecting electron diffraction data for PDF analysis:

Energy filtering. Traditionally, electron diffraction data for PDF analysis are collected using energy filtering in order to exclude the inelastic scattering contribution. However, quantitative or semi-quantitative electron PDFs can be obtained without filtering (Abeykoon *et al.*, 2012).

Multiple scattering/dynamical effects. In order to keep the contribution of non-kinematic scattering low, the sample thickness and the nanoparticle size should be as small as possible. Generally, particles 10 nm and smaller should scatter kinematically, and this is the size range that benefits most from PDF analysis (Abeykoon *et al.*, 2012).

Powder average. Proper statistics are important for PDF analysis. In order to decrease measurement errors one can increase the illumination area on the sample (or the selected-area aperture in the case of SAED), collect several diffraction patterns from different areas and average them.

Scattering angle range. A large θ range is essential for PDF analysis. An electron diffraction experiment offers significant flexibility in selecting the scattering range through the adjustment of the electron diffraction camera length and illumination wavelengths. Additionally, in order to enhance the data quality, merging of different scattering ranges recorded in a set of diffraction patterns is possible (Petersen *et al.*, 2005).

An electron diffraction pattern is a combination of signals produced by *elastically* and *inelastically* scattered electrons. The inelastic component is a result of electron energy loss due to plasmon or inner-shell excitation, electron Compton or thermal diffuse scattering (Egerton, 2011). For crystalline materials with distinct Bragg peaks the inelastic scattering is not particularly critical, as it mainly contributes to the background in diffraction patterns and can be neglected when only the intensities of the Bragg peaks are analysed. For PDF analysis the total scattering profile is used; thus, the inelastic scattering, which can significantly modify the scattering profile, needs to be considered (Ishimaru, 2006). Two strategies are followed in this respect: (i) energy filtering of diffraction patterns, which is the more accurate approach but demands specific instrumentation, and (ii) subtraction of the background scattering taken from an area adjacent to the sample (*i.e.* from the supporting film), which assumes that the main inelastic scattering component originates from the support, and the contribution from the sample can be neglected (Cockayne, 2007). The validity of this approximation depends on the level of quantification intended in the particular study.

The PDF formalism presented above is based on the single-scattering approximation. Multiple scattering, which is much stronger in electron diffraction than for X-rays and neutrons, significantly affects the total scattering profile and therefore the PDF. The multiple-scattering effects can modify the peak positions in the PDF as well as the relative intensities of the peaks, the latter being more sensitive to multiple scattering (Anstis *et al.*, 1988). It has been shown that for amorphous materials, owing to the contribution of the multiple scattering, the total scattering profile depends on the thickness of the foil (Childs & Misell, 1972; Rez, 1983). Knowledge of the film thickness allows extraction of the single-scattering distribution. An improved agreement with the expected PDF was shown for hydrogenated amorphous silicon (Anstis *et al.*, 1988) and amorphous germanium (Ankele *et al.*, 2005) using the single-scattering profile.

Experimentally, it is difficult to determine the sample thickness along the incident-electron-beam direction. In this case, the thickness parameter employed in calculations can be varied, adjusting the amplitudes of the PDF. An estimate for the sample thickness is found when the optimal fit is obtained. Different input values of the thickness result in different principal gradients of the oscillations. Once a reasonable fit is found, the correct thickness is determined and the contribution of multiple scattering can be eliminated (Ankele *et al.*, 2005). This method was